ECCOMAS Congress 2016
VII European Congress on Computational Methods in Applied Sciences and Engineering
M. Papadrakakis, V. Papadopoulos, G. Stefanou, V. Plevris (eds.)
Crete Island, Greece, 5–10 June 2016

EFFECT OF THE SEISMIC EXCITATION'S INCIDENCE ANGLE ON THE NONLINEAR BEHAVIOR OF BASE ISOLATED BUILDINGS CONSIDERING POUNDING TO ADJACENT MOAT WALLS

Eftychia A. Mavronicola[1*], Panayiotis C. Polycarpou[2], and Petros Komodromos[1]

[1,3] Department of Civil and Environmental Engineering, University of Cyprus
75 Kallipoleos Street, P.O. Box 20537, 1678 Nicosia, Cyprus
mavronicola.eftychia@ucy.ac.cy, *komodromos@ucy.ac.cy*

[2] Civil and Environmental Engineering Program, Department of Engineering, University of Nicosia
46 Makedonitissas Avenue, P.O. Box 24005 1700 Nicosia, Cyprus
polycarpou.p@unic.ac.cy

Keywords: pounding, non-linear analysis, three-dimensions, adjacent structures.

Abstract. *In the last decades, a number of reconnaissance reports have revealed that pounding between adjacent buildings, during strong earthquakes, may induce local and in some extreme cases severe structural damage. The problem of earthquake-induced pounding of adjacent buildings has been the subject of great scientific interest, while several recent numerical studies have quantified the effects of seismic pounding of buildings, with the majority of researchers simulating the problem in two dimensions (2D). The results from the various 2D parametric studies have demonstrated the potentially detrimental effects of pounding on the dynamic response of multistory buildings and revealed the importance of this problem regarding the safety and functionality of colliding structures. Furthermore, most of the numerical studies have been limited to the utilization of linear elastic structural models to simulate the adjacent buildings. The current study parametrically investigates the effect of pounding on the inelastic response of base isolated structures, which are simulated as non-linear 3D multi-degree of freedom systems subjected to bidirectional earthquake excitations. Specifically, the influence of certain parameters, such as the angle of the seismic incidence, the width of the seismic gap, characteristics of the isolation system and the configuration of the adjacent structures on the peak response, is parametrically examined, for various near-fault excitations. All numerical simulations are performed using a specially developed software that implements an innovative, simple and efficient approach to model impacts in 3D, taking into account the arbitrary location of contact points and the geometry at the vicinity of impact.*

1 INTRODUCTION

Frequently, neighboring buildings are constructed very close to each other, sometimes without any clearance between them. Hence, structural poundings may inadvertently occur between adjacent buildings, due to deformations of their stories, during strong seismic excitations. Consequences of such pounding incidences, ranging from local light damage to severe structural damage or even collapse, have been observed and reported after severe earthquakes. Poundings may also occur even in cases of seismically isolated buildings when the width of the available seismic gap around them is relatively limited, due to the large horizontal relative displacements that are expected at the isolation level, especially during near-fault, pulse-like ground motions.

Although several research studies have been conducted in order to investigate the problem of earthquake-induced poundings of adjacent structures and its consequences, most of them have been limited to simplified planar (2D) analyses [1–6], apparently due to the involved complexities and the consequently excessive computational cost. However, the effect of crucial factors, such as the consideration of both orthogonal seismic components, friction phenomena that occur during pounding, non eccentric impacts, irregularities, or asymmetries in the plan view of the colliding structures, which may excite the torsional vibration of a building and further increase the possibility of impacts during earthquakes, are essential parameters that can be taken into account only through three-dimensional (3D) simulations.

Recently, some researchers have shown great interest on the exploration of the effects of earthquake induced pounding of seismically isolated structures using 3D nonlinear dynamic analyses [7–12]. More specifically, Matsagar and Jangid, 2010 [7] investigated the seismic response of a single-story asymmetric structure supported on various base isolation systems during impact with adjacent structures. The effects of impact were found to be severe for systems with flexible superstructure, stiffer adjacent structures and increased eccentricities. Pant and Wijeyewickrema, 2014 [11] used a three-dimensional finite element model in order to investigate the seismic performance of a four-story building under bidirectional far-fault non-pulse-like and near-fault pulse-like ground motions scaled to represent two levels of shaking. Seismic pounding of the building with the retaining walls at its base was simulated using a specially developed purpose contact element that accounts for friction. Polycarpou *et al.*, 2015 [13] considered a new methodology for simulating earthquake induced pounding of seismically isolated buildings that are modeled as 3D multi-degree-of-freedom (MDOF) systems. An example of a 3-story seismically isolated building, pounding against the surrounding moat wall, has been presented to demonstrate the advantages of the proposed methodology.

The current study, utilizing the methodology described in [13, 14], aims to thoroughly investigate the circumstances under which spatial poundings may occur and assess the effect of some important parameters on the peak structural response considering pounding incidences. Nonlinear time-history analyses are carried out considering the arbitrary direction of the ground motion with respect to the structural axes of the simulated structures. The influence of the isolator's characteristics, the superstructure stiffness and the separation distance between the building and the retaining walls at its base is also investigated, while considering different geometrical arrangements for the moat walls.

2 MODEL FOR SIMULATION OF SEISMIC POUNDING

The numerical simulation of 3D pounding enables the investigation of certain parameters that are associated with the spatial movement of the seismically isolated building and cannot be explored through planar dynamic analyses. The effects of seismic pounding on the response of base-isolated reinforced concrete buildings under bidirectional excitations are

hereby investigated. A 3D model of a base isolated building is considered, where a recently proposed methodology [13, 14], which takes into account the arbitrary location of impacts and the geometry at the point of impact, is used. In particular, a new approach to the numerical problem of spatial impact modeling that does not require the a priori determination of the contact points was presented, taking also into account the geometries of the colliding structures at the vicinity of an impact.

More specifically, the simulated base isolated buildings are modeled as 3D-MDOF systems with shear-type behavior for their superstructures in the horizontal directions. The slab at each floor level of the superstructure is represented by a rigid diaphragm that is mathematically simulated as a convex polygon, while the masses are considered to be lumped at the floor levels, having three dynamic degrees of freedom (DOFs), i.e. two translational, parallel to the horizontal global axes, and one rotational along the vertical axis. Thus, considering ground excitations only in the horizontal directions, which is the most important case, no displacements occur in the vertical direction, since the translational dynamic DOFs of the structure refer only to horizontal planes. Consequently, it is assumed that the impact forces occur only in horizontal planes.

The time-history analysis involves the numerical integration of the differential equations of motion at each time step and the calculation of the resulting displacements, velocities and absolute accelerations at each DOF of each building. Based on the deformed position of each floor diaphragm in the 3D space, an automatic contact detection check is performed to identify potential contacts between structures, which are subsequently used for the computation of appropriate impact forces to be applied at the corresponding DOFs.

The majority of the force-based impact models that are available in the scientific literature calculate the impact force as a function of the interpenetration depth between the colliding bodies. However, the usage of the interpenetration depth as the key variable constitutes a significant drawback in the case of 3D impact modelling, as it cannot correctly assess the proper values of the impact forces. Therefore, in the proposed methodology, the area of the overlapping region, instead of the interpenetration depth, is used as the key variable in the calculation of the impact forces. Figure 1 describes, schematically, how the proposed impact model works. In particular, when two slabs, which are modelled as polygons, come in contact, they form an overlapping region that is either a triangle or a quadrilateral. The algorithm uses the geometry of the overlapping area at each time step in order to determine the location of the action point of the impact forces, as well as the direction and the magnitude of the impact forces. The Coulomb law of friction restricts the magnitude of the tangential impact force below a certain value.

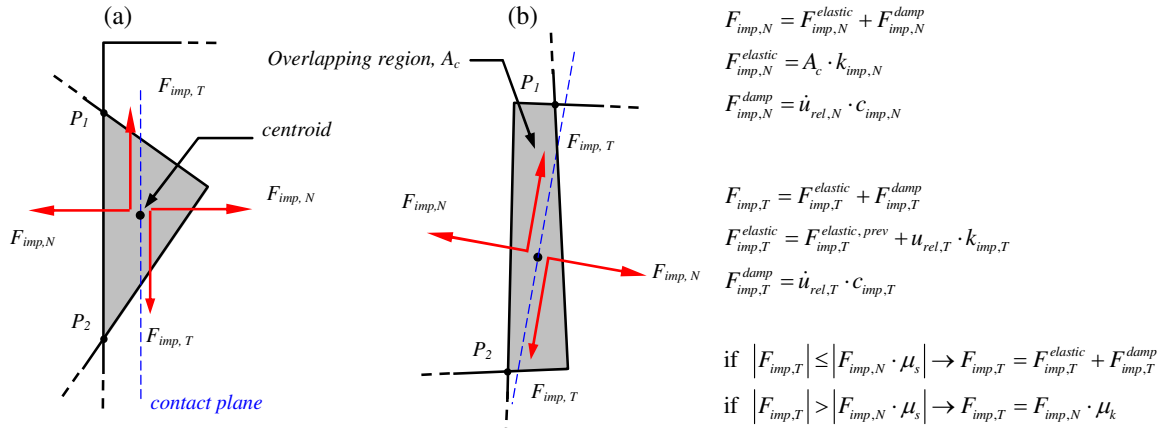

Figure 1: Schematic representation of the contact plane, based on the geometry of the indentation region, which can be either (a) a triangle, or (b) a quadrilateral.

3 DATA ANALYSIS

A three-storey (three-bay by three-bay), base-isolated reinforced concrete moment-frame building is chosen as a typical model structure (Figure 2). The building is symmetric with coinciding centers of mass and stiffness. The retaining walls extend from the ground level up to the base level of the building. All column sections of the simulated building have square dimensions of 45 x 45 cm^2. The bay width of the building in both directions is 5.5 m while each storey height is 3.2 m. The elastic modulus of concrete is assumed to be 30 GPa with a Poisson's ratio of 0.2. A uniformly distributed mass of 250 tons is considered for the roof mass, while a 340 tons floor mass is assumed at each other floor level, including the base of the building. For the determination of the Rayleigh damping matrix, the viscous damping ratios for the first and the fourth eigenfrequencies are taken as 0.05 and 0.02, respectively. Due to symmetry, the first two eigenmodes are translational along the two horizontal axes. The fundamental eigenperiods of the corresponding conventionally fixed-supported building are: $T_{x,fixed} = T_{y,fixed} = 0.311\sec$.

A coupled plasticity model is used for simulating the bidirectional lateral response of the seismic isolators. The aforementioned model is based on the hysteretic behavior proposed by Wen, 1976 [15] and Park *et al.*, 1986 [16] and recommended by Nagarajaiah *et al.*, 1991 [17]. Here, for each bearing element an isolation period based on the post-yield stiffness of 2.0 seconds, a yield displacement equal to 1.0 cm and a normalized characteristic strength $F_{xi}^{x}/W = F_{yi}^{y}/W$ equal to 0.05 or 0.10 are considered.

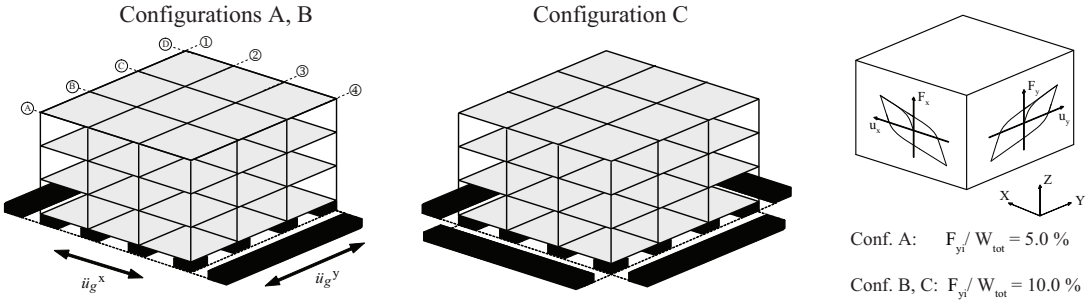

Figure 2: Configurations considered in the present study.

Impacts occur at the isolation level when the clearance from the surrounding moat wall, i.e. the seismic gap, is exceeded, during very strong seismic excitations. Nevertheless, the methodology provides the ability of considering impacts at all floor levels of the seismically isolated building in case of pounding with other adjacent buildings. The moat wall is modeled as a single-mass system, with three dynamic DOF, as in the case of a single-storey structure. The moat wall is taken to be 100 cm thick and 100 cm high, resulting in a substantially stiff barrier, while it's mass is assumed to be 5 tons/m, a number that takes into account the contribution of the backfill soil. The normal impact stiffness is $k_{imp,N}=2.58\times10^7$ *kN/m*^{2}, while the corresponding tangential impact stiffness is $k_{imp,T}=5.74\times10^6$ *kN/m*. The static and kinetic friction coefficients are taken as $\mu_s = 0.8$ and $\mu_k = 0.6$, respectively.

A set of earthquake ground motions has been selected from the Pacific Earthquake Engineering Research Center database. The selected seismic accelerograms (Table 1) are expected to induce large relative displacements to the seismically isolated building, since they are characterized by low-frequency contents, which is one of the most decisive factors for the occurrence of pounding in such structures. The response spectra of the five earthquakes' fault-

normal (FN) and fault-parallel (FP) components that have been used in this study are plotted in Figure 3.

NGA	Event	Year	Station	Mw	Comp	PGA (g)	PGV (cm/s)	PGD (cm)
#779	Loma Prieta	1989	LGPC	6.93	FN	0.94	97	62.5
					FP	0.54	72.1	30.5
#821	Erzican- Turkey	1992	Erzincan	6.69	FN	0.49	95.4	32.1
					FP	0.42	45.3	16.5
#828	Cape Mendocino	1992	Petrolia	7.01	FN	0.61	81.9	25.5
					FP	0.63	60.4	26
#1084	Northridge-01	1994	Sylmar – Converter Sta	6.69	FN	0.59	130.3	54
					FP	0.8	93.3	53.3
#2627	Chi-Chi- Taiwan-03	1999	TCU076	6.2	FN	0.52	59.3	9.6
					FP	0.16	19.5	3.6

Table 1: Summary of the main characteristics of the selected horizontal seismic excitations.

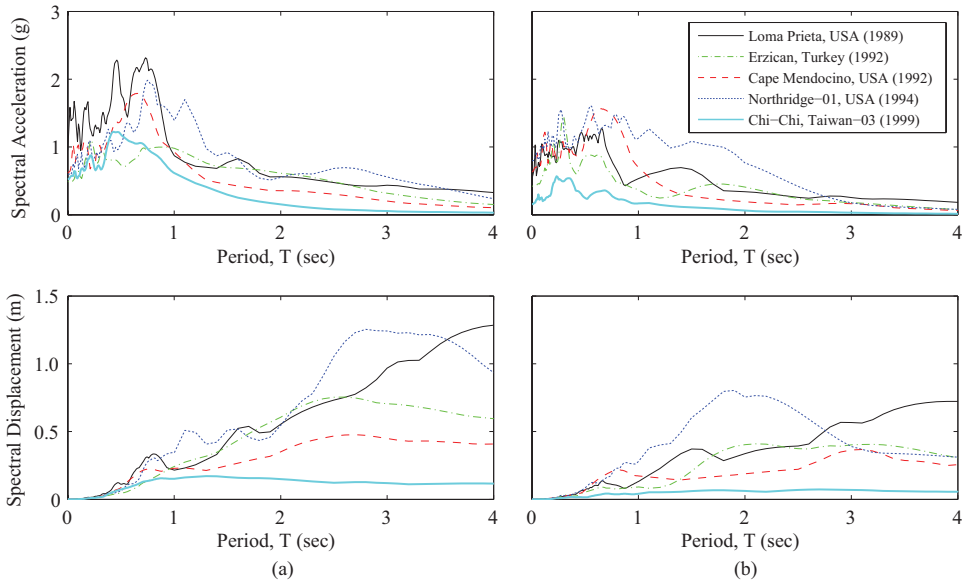

Figure 3: Acceleration and displacement response spectra of the (a) fault-normal, and (b) fault-parallel seismic components of the 5 earthquake records, considering a viscous damping ratio of 5 %.

4 INFLUENCING FACTORS IN 3D SIMULATIONS

The effect of the angle of incidence, on the peak structural response of the previously described 3-storey base isolated building, is presented in this section. The simulated structures are subjected, simultaneously, to two orthogonal, horizontal seismic excitations of their supporting ground. By rotating each of the 5 seismic record pairs, as presented in Table 1, from 0° to 180°, with respect to the system's principle axes of construction, with a 5° interval in the clockwise direction, one can consider 37 alternative excitation cases. In order to identify potential differences in the response of a 3-storey building due to the angle of incidence of the ground motion, the half polar plots of peak interstorey drifts are plotted in Figure 3, considering the Loma Prieta and the Northridge earthquakes. Specifically, the peak responses are presented for different characteristics of the seismic isolation system in Figure 4(a) and (b), for both seismic excitations. It is observed that the interstorey drifts tend to decrease with an increase in the normalized characteristic strength of the isolation system, Figure 4(b).

The simulation results indicate that the maximum responses occur at different angles. The critical angle in the longitudinal (*E-W* or *X*) direction is not always at 0 and 90 degrees, but occurs in incidental angles that are quite different for each excitation. In the case of seismically isolated buildings, the maximum relative displacements at the isolation level in the *X*-direction can vary by a factor of 3.9 and 1.4 over the possible angles of interest, for the Loma Prieta and the Northridge earthquakes, respectively. This is considered to be a significant variation. For both excitations, the critical excitation angle for the interstorey deflections is nearly common among all floors. The maximum floor relative displacement in the *X*- direction occurs at the complimentary angle of the maximum interstorey drift in the *Y*- direction. Although, the peak interstorey drifts in each direction depend highly on the incidence angle, the vector sum of the responses (i.e. the vectorial summation of the peak responses in the Cartesian Coordinates X and Y) slightly varies for different angles. As the peak responses of the X and Y components occur at different time intervals, although their vectorial summation does not have a physically meaning nevertheless it provides a conservative upper bound limit that can be used for design purposes.

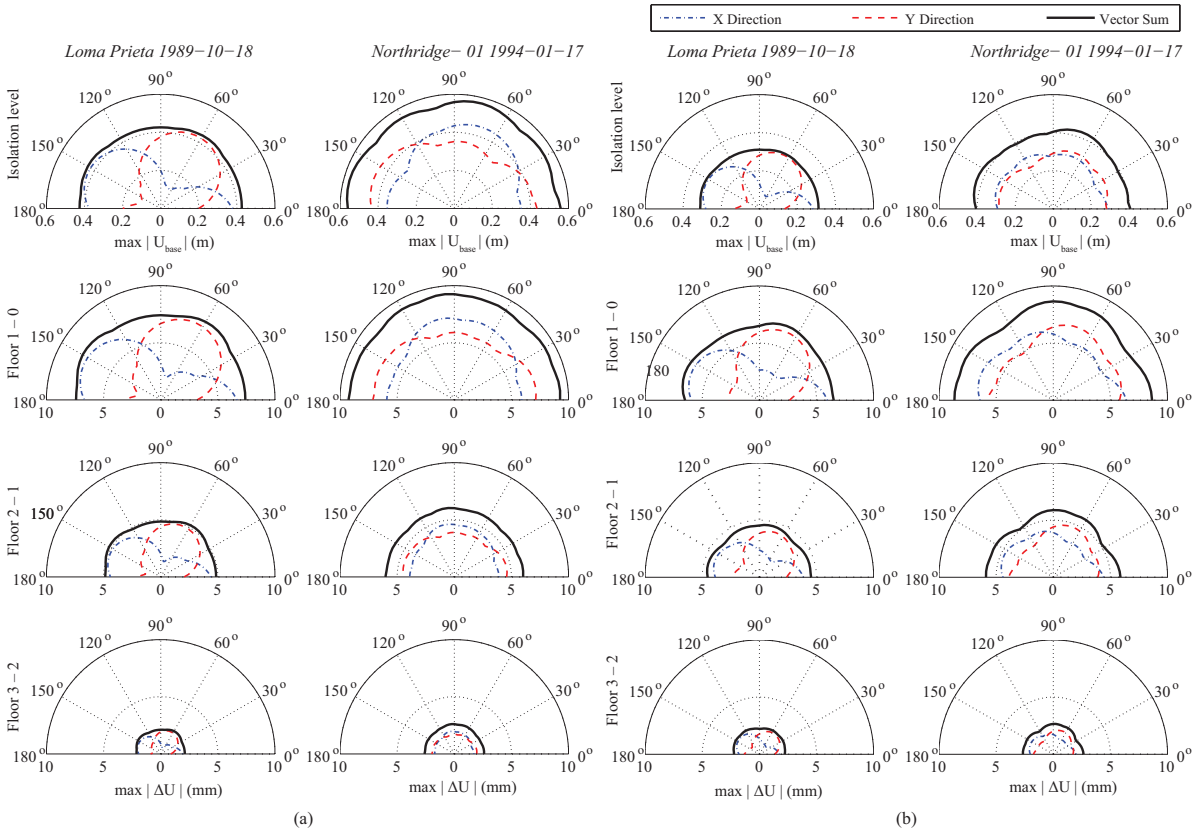

Figure 4: Peak responses of the buildings' corner column A_1 as a function of the angle of incidence considering the no pounding" case, for seismic isolation systems with T_b = 2.0 sec, u_y = 1.0 cm, F_{yi}/W_{tot} equal to (a) 0.05 and (b) 0.10; in both directions.

4.1 Isolator characteristics and configuration

Peak absolute values of the base drifts and the envelope of interstory deflections of the column A_1, are shown in Figures 5 and 6 for various angles of seismic incidence. For the analyses, both FN/FP components of the five selected near-fault ground motions are simultaneously used. The seismic gap is assumed to be 20 cm for the four of the selected exci-

tations and 10 cm for the remaining (Chi-Chi- Taiwan-03) ground motion. Three configurations are considered (Figure 2), as follow:

Conf. A: Base-isolated building with retaining walls in two sides (*E-W* direction)
LRBs: $T_b^x = T_b^y = 2.0$ sec, $u_y^x = u_y^y = 1.0$ cm, $F_{yi}^x / W = F_{yi}^y / W = 5.0\%$

Conf. B: Base-isolated building with retaining walls in two sides (*E-W* direction)
LRBs: $T_b^x = T_b^y = 2.0$ sec, $u_y^x = u_y^y = 1.0$ cm, $F_{yi}^x / W = F_{yi}^y / W = 10.0\%$

Conf. C: Base-isolated building with retaining walls in all four sides
LRBs: $T_b^x = T_b^y = 2.0$ sec, $u_y^x = u_y^y = 1.0$ cm, $F_{yi}^x / W = F_{yi}^y / W = 10.0\%$

In this section, the response of the base-isolated building in each configuration is discussed. The results for the "no pounding" case are presented in Figure 5, and, for comparison purposes, the restricted base drifts of the corner column are also plotted for each excitation in terms of the excitation angle. The variation of the unobstructed base drifts indicate that the value of the incidence angles depends on the characteristics of the earthquakes, in combination with the characteristics of the isolation system. The critical excitation angle of a certain response quantity differs among the various earthquakes.

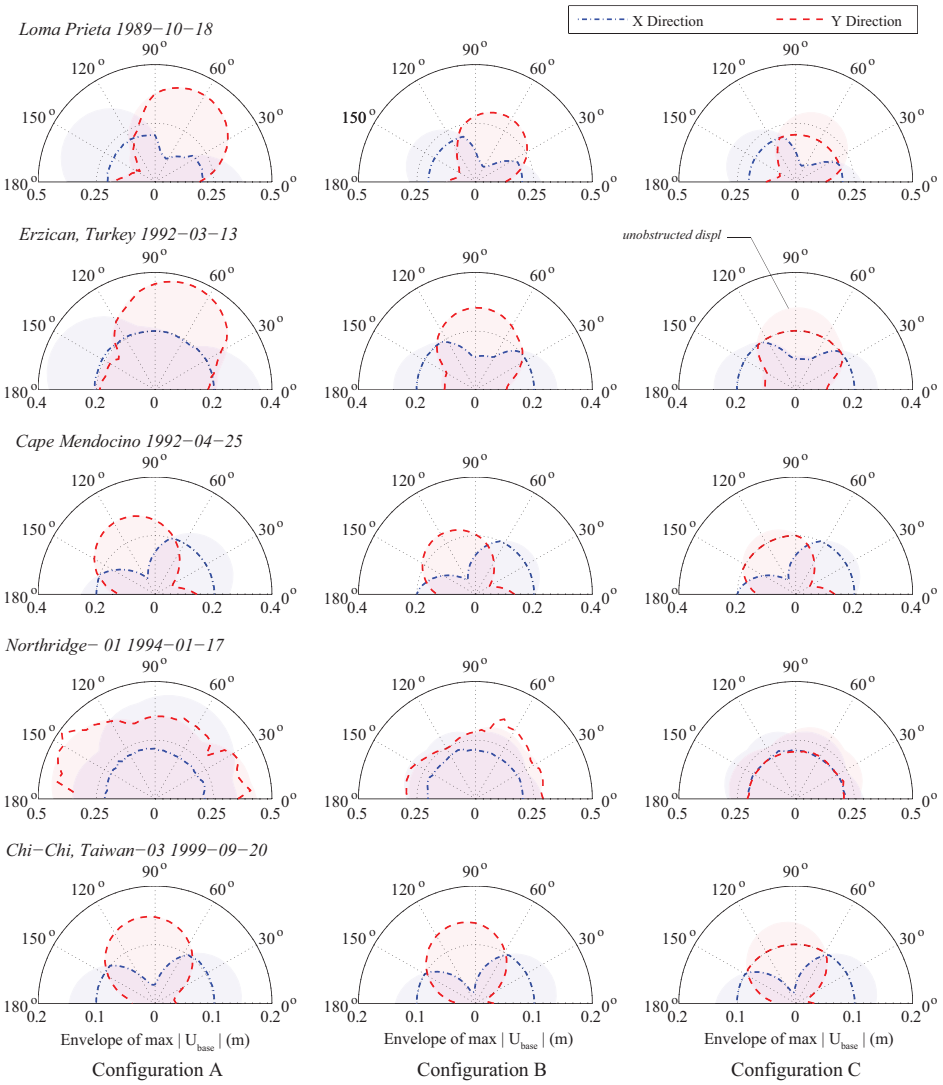

Figure 5: Half-polar plots of maximum unobstructed and restricted relative displacements at the isolation level of the buildings' corner columns in terms of the excitation angle for different configurations.

The peak responses of the superstructure of the base isolated building considering different configurations and the corresponding fixed-supported building without pounding are presented in Figure 6. It becomes evident from the computed results, that the direction of the seismic excitation affects substantially the maximum response of the seismically isolated building, especially during pounding with the surrounding moat walls. The increase in drift demands due to pounding in Configuration B is less compared to Configuration A for all examined ground motions (second and third columns of Figure 6). This is mainly because the available gap size is more restricted in the first case compared to the corresponding maximum unobstructed displacement of the base isolated building, as illustrated in the first two columns of Figure 5.

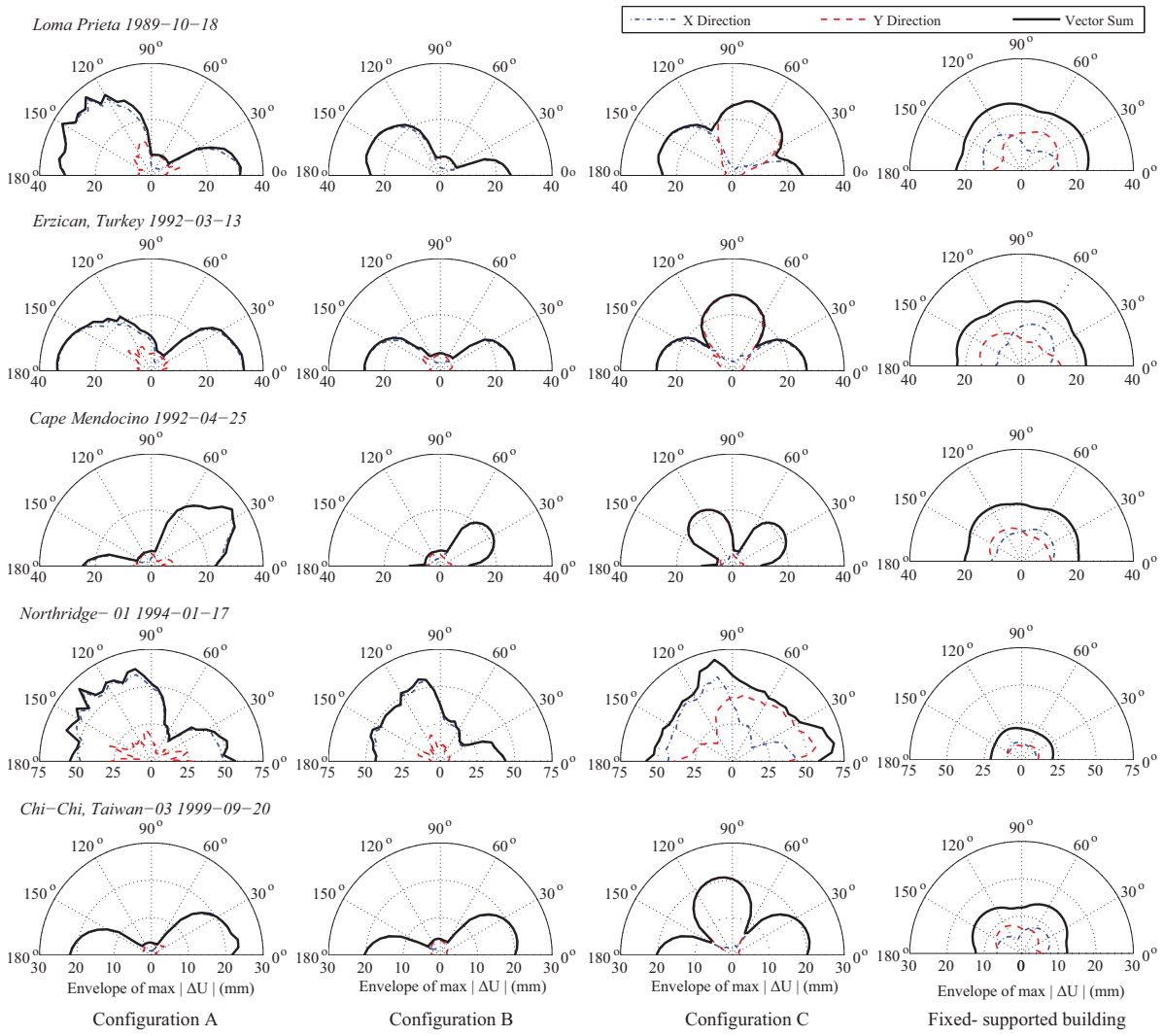

Figure 6: Envelope of peak interstorey drifts of the buildings' corner column A_1 in terms of the excitation angle, considering the pounding case with the moat wall for various configurations; under five near-fault ground motions, and the no pounding case of a conventionally fixed-supported building.

For the configurations A and B, due to poundings with the moat walls at the *X*-direction, if we consider 360°, due to the rotational symmetry of the 180° plots, the plots of the peak responses would resemble 8-shapes, exhibiting a pronounced dependence of the peak response on the incidence angle. Furthermore, the change in the response–angle relationship due to pounding is not so obvious in the *Y*-direction, since impacts occur only in the *X*-direction. For

the Configuration C, the peak response depends on the incidence angle, and the maximum interstorey drifts tend to exhibit two maxima in orthogonal directions. Furthermore, although the retaining walls are placed on each of the four sides of the building, four of the excitations resulted in one-direction impact for a range of excitation angles leading to a petal-like shape response, with two-orthogonal axes of symmetry. For example, for the Loma Prieta excitations, considering an incidence angle, $\theta \approx 30\text{-}100^\circ$, impacts occur only in the *Y*-direction.

The maximum interstorey drift over all examined orientations seems to be polarized in the direction in which the peak base displacement is observed; this polarization is almost perfect for this symmetric-plan building. The value of the maximum inter-storey drift ratio, due to the Northridge earthquake, indicates potential collapse of the first storey. Drift demands due to other earthquakes are significantly lower for all the cases that have been examined. As already discussed, the influence of poundings in the response of the base isolated building can be much less detrimental when isolators with normalized characteristic strength equal to 0.10 are incorporated, however the peak interstorey drifts due to impacts can become higher than those for the corresponding fixed-supported building (as shown in the last column of Figure 6).

4.2 Available gap size

In order to examine the effect of the seismic gap size on the response of the seismically isolated building during pounding with the moat wall, two of the aforementioned configurations are considered. The structural characteristics of the base isolated buildings, as well as the isolation characteristics are kept the same. The width of the seismic gap varies from 15 to 35 cm, with a step of 2.5 cm. Figures 7 (a) and (b) show the relationship among peak interstorey drifts of the 3-storey seismically building, the incidence angle and the width of the available seismic gap of the adjacent walls located in the *E-W* direction under the bidirectional excitation of the Loma Prieta and the Northridge earthquakes, respectively. Similarly organized results are presented in Figure 8, considering impacts with the surroundings walls located around all four sides of the simulated building.

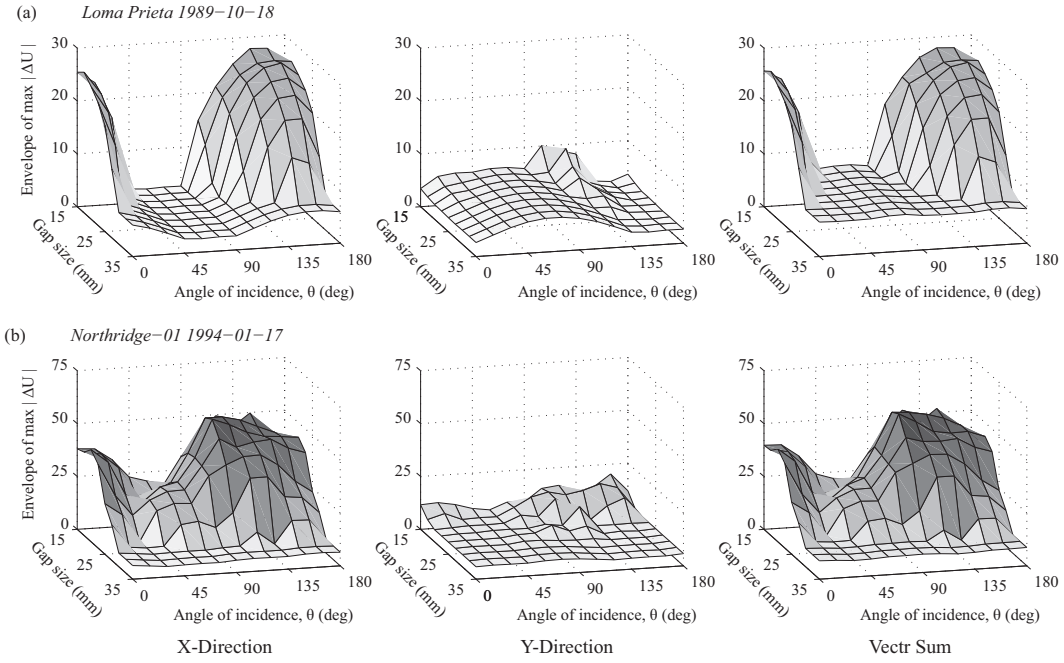

Figure 7: Envelope of the interstory deflections in the X and Y directions, as well as vector sum for different combinations of the excitation angle and the available gap size, considering adjacent walls in the two sides of the building (Conf. B) for (a) the Loma Prieta, and (b) the Northridge excitations.

It becomes evident from the plots, that the angle for which the maximum response is observed is not the same for the two earthquakes that are considered, while the degree by which pounding affects the peak response seems to depend on the ground motion characteristics and the available gap size. The influence of the excitation angle is more pronounced in the case of pounding in one direction, as shown in Figure 7. Furthermore, it is important to mention that although no pounding occurs in the *Y*-direction the deflections of the column A_1 in the Y direction are also considerably affected from pounding in cases with more restricted gap in the *E-W* direction. In general, the vector sum of the superstructure' drifts increases when the separation distance between structures decreases and, then, slightly decreases with further reduction in the separation. It is noteworthy that the interstorey drifts in the X and Y directions, as shown in the first two columns of Figure 8, respectively, present translational symmetry. Furthermore, translational symmetry seems to appear to the vector sum of interstorey drifts due to the bilateral symmetry of the building and the adjacent structures.

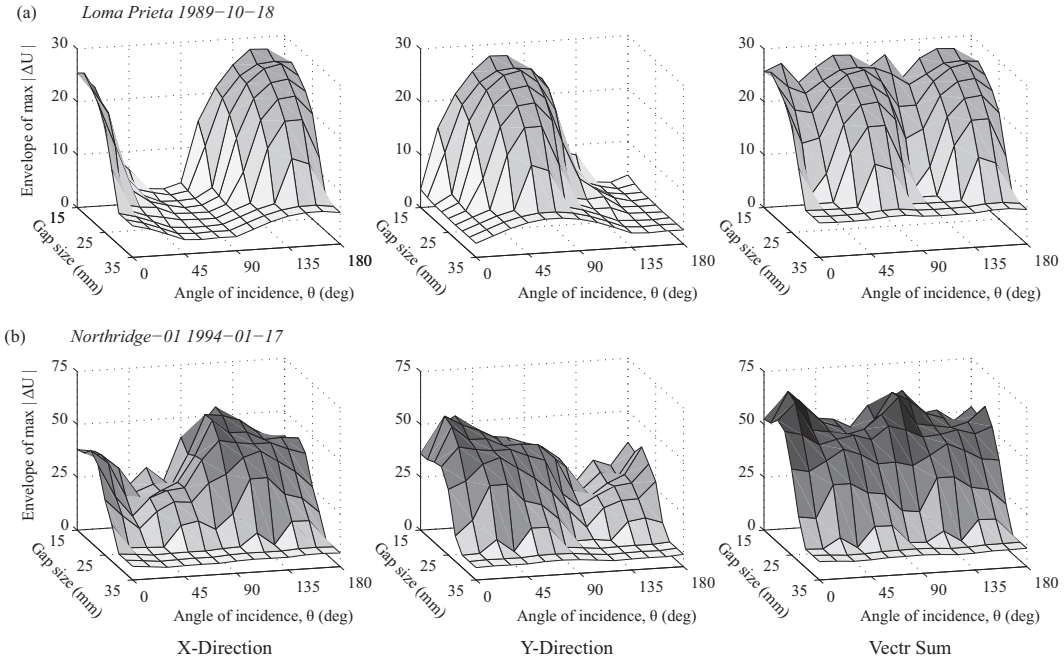

Figure 8: Envelope of the story drifts for various excitation angles and gap sizes for Configuration C under near fault ground motions.

4.3 Stiffness of the superstructure

In order to study the effects of the superstructure's flexibility on the overall dynamic response, the peak interstorey drifts are obtained for different fundamental eigenperiods of the superstructure of the examined three-storey isolated building with impact conditions under the Loma Prieta and Northridge earthquakes, as shown in Figure 9. Different superstructure's stiffnesses are obtained considering different cross sections of the columns. The isolation system considered consists of lead-rubber bearings (LRBs) with normalized characteristic strength $F_{yi}^{x}/W = F_{yi}^{y}/W$ of 0.10 in both directions, with isolation gap distances of 20 cm around all four sides of the structure. It should be noted that the results presented in Figure 9(b) refer to the peak response of the previous section described in Configuration C.

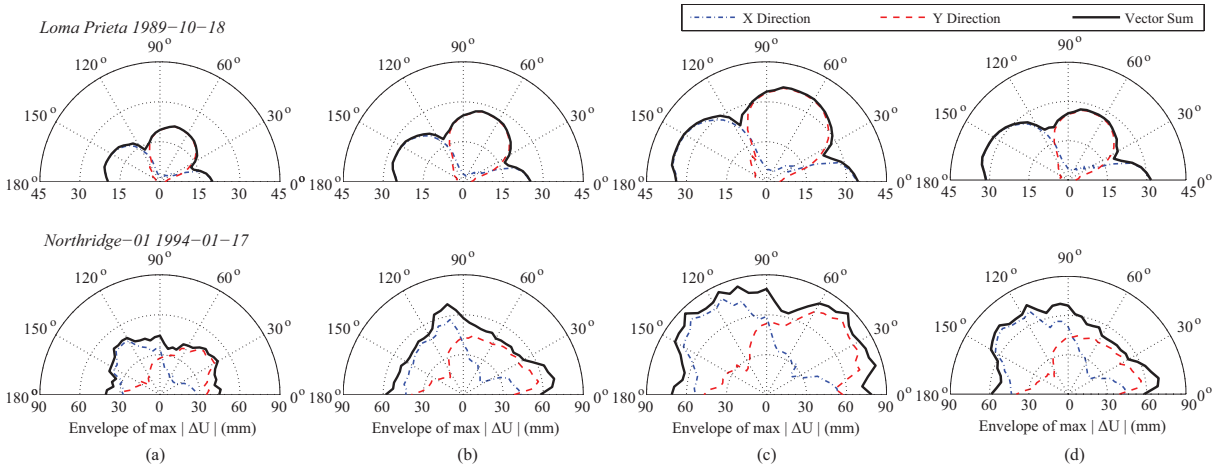

Figure 9: Envelope of peak interstorey deflections of the buildings corner columns in terms of the excitation angle considering superstructure stiffness: $T_{x,\,fixed} = T_{y,\,fixed}$ equal to (a) 0.25 sec, (b) 0.311 sec, (c) 0.394 sec, and (d) $T_{x,\,fixed} = 0.372$ sec, $T_{y,\,fixed} = 0.312$ sec.

These figures show that the superstructure's deflections undergo an increase when the fundamental eigenperiod of the corresponding superstructure increases. This implies that the behavior of the base isolated building during impact becomes adverse while increasing the flexibility of the superstructure. Furthermore, the stiffness of the superstructure does not seem to influence the excitation angle that dominates the response. It is possible to identify a clear pattern in the response of the structure. For structures with equal horizontal stiffness along the two axes of symmetry X and Y, where $T_{x,\,fixed} = T_{y,\,fixed}$, the response shows two separate peaks for the Loma Prieta excitation, one associated with $\theta = 75°$ and the second around $\theta = 165°$, leading to a petal-like shape with double symmetry. For the structures with unequal eigenperiod, instead, the peak tends to be in a single direction, and the plots assume a shape with unequal "petal" length. Furthermore, there is a similar response of the interstorey deflections in *Y*-direction in Figure 9(b) and (d), for both excitations, which relates to the almost identical superstructure stiffness in Y-direction.

5 CONCLUSIONS

The present study demonstrates the importance of implementing an efficient methodology with simple structural and impact modelling in three dimensions, in order to investigate the seismic pounding on the response of MDOF systems. Seismic response of a 3-storey base isolated building during impact with an adjacent moat wall is investigated. The comparative performance of different isolation systems during various impact conditions is studied under five near-fault ground motions. Parametric studies for simulating earthquake induced pounding of seismically isolated buildings are conducted in three-dimensions to observe the influence of the incidence angle, the width of the seismic gap and the flexibility of the superstructure on the peak response of the base isolated building. From the trend of the results presented hereby, the following conclusions are drawn:

- The deflection of the superstructure of a base-isolated building increases significantly when impact with a moat wall takes place during an earthquake. The bearing displacement is consequently reduced.
- The detrimental effects of pounding may become more severe for certain values of the excitation angle. The incidence angle, in which the amplification of the superstructure response due to pounding with the adjacent building obtains its maximum value, generally coincides with the angle in which the peak base displacement occurs.

- In general, the degree by which the incidence angle affects the interstory deflections seems to be significantly affected by the surrounding wall arrangement.
- The normalized characteristic strength of the isolators has significant influence on the peak response of a base-isolated structure during impact. This can be justified considering that with an increase of the F_{yi}/W_{tot} ratio, the relative displacements at the isolation level decrease substantially, in combination to the influence of the width of the available seismic gap compared to the corresponding maximum unobstructed displacements under those excitations.
- As the seismic gap between the base-isolated building and the adjacent wall decreases, there is an increase in the deflections of the superstructure up to a certain value of the gap distance and, then, onwards the deflections of superstructure decrease.
- Increased flexibility of the superstructure increases significantly the drifts of the superstructure during impact with the adjacent structure.

REFERENCES

[1] Matsagar, V. A.., Jangid, R. S., Seismic response of base-isolated structures during impact with adjacent structures. Eng. Struct. **25**(10), 1311–1323, 2003.

[2] Komodromos, P., Simulation of the earthquake-induced pounding of seismically isolated buildings. Comput. Struct. **86**(7-8), 618–626, 2008.

[3] Ye, K., Li, L.., Zhu, H., A modified Kelvin impact model for pounding simulation of base-isolated building with adjacent structures. Earthq. Eng. Eng. Vib. **8**(3), 433–446, 2009.

[4] Polycarpou, P. C.., Komodromos, P., On poundings of a seismically isolated building with adjacent structures during strong earthquakes. Earthq. Eng. Struct. Dyn. **39**(8), 933–940, 2010.

[5] Mavronicola, E., Polycarpou, P. C.., Komodromos, P., The effect of modified linear viscoelastic impact models in the pounding response of a base-isolated building with adjacent structures. *5th ECCOMAS Thematic Conference on Computational Methods in Structural Dynamics and Earthquake Engineering* (COMPDYN2015), Crete, 2015

[6] Jankowski, R.., Mahmoud, S., *Earthquake-Induced Structural Pounding,* Springer International Publishing, Cham, 2015.

[7] Matsagar, V. A.., Jangid, R. S., Impact Response of Torsionally Coupled Base-isolated Structures. J. Vib. Control **16**(11), 1623–1649, 2010.

[8] Sato, E., Furukawa, S., Kakehi, A.., Nakashima, M., Full-scale shaking table test for examination of safety and functionality of base-isolated medical facilities. Earthq. Eng. Struct. Dyn. **40**(13), 1435–1453, 2011.

[9] Jankowski, R., Non-linear FEM analysis of pounding-involved response of buildings under non-uniform earthquake excitation. Eng. Struct. **37**, 99–105, 2012.

[10] Varnava, V.., Komodromos, P., Assessing the effect of inherent nonlinearities in the analysis and design of a low-rise base isolated steel building. Earthq. Struct. **5**(5), 499–526, 2013.

[11] Pant, D. R.., Wijeyewickrema, A. C., Performance of base-isolated reinforced concrete buildings under bidirectional seismic excitation considering pounding with retaining walls including friction effects. Earthq. Eng. Struct. Dyn. **43**(10), 1521–1541, 2014.

[12] Moustafa, A.., Mahmoud, S., Damage assessment of adjacent buildings under earthquake loads. Eng. Struct. **61**(1), 153–165, 2014.

[13] Polycarpou, P. C., Mavronicola E., Komodromos, P., Planar and spatial numerical investigation of the effects of earthquake-induced pounding of base isolated buildings. *14th World Conference on Seismic Isolation, Energy Dissipation and Active Vibration Control of Structures* (14WCSI), San Diego, Ca USA, 2015.

[14] Polycarpou, P. C., Papaloizou, L.., Komodromos, P., An efficient methodology for simulating earthquake-induced 3D pounding of buildings. Earthq. Eng. Struct. Dyn. **43**(7), 985–1003, 2014.

[15] Wen, Y.-K., Method for random vibration of hysteretic systems. J. Eng. Mech. Div. **102**(2), 249–263, 1976.

[16] Park, Y. J., Wen, Y.-K.., Ang, A., Random vibration of hysteretic systems under bi-directional ground motions. Earthq. Eng. Struct. Dyn. **14**(4), 543–557, 1986.

[17] Nagarajaiah, S., Reinhorn, A. M.., Constantinou, M. C., Nonlinear Dynamic Analysis of 3D Base Isolated Structures. J. Struct. Eng. **117**(7), 2035–2054, 1991.